Dynamics of Propene Metathesis: Physisorption and Diffusion in Heterogeneous Catalysis

Vincent G. Gomes and O. Maynard Fuller
Dept. of Chemical Engineering, McGill University, Montréal, Canada

Simultaneous effects of physisorption, diffusion, and reaction were characterized by dynamic experiments for propene metathesis over rhenium oxide/γ-alumina catalyst in a Berty reactor. Single-component sorption isotherms from steady-state experiments for ethene, propene, and 2-butene were used to predict multicomponent physisorption by the ideal adsorbed solution theory. Effective diffusivities were determined from molecular, Knudsen, and surface-diffusion coefficients, including bimodal pore-size effect and tortuosity factors. Transient sorption diffusion experiments were conducted with inactivated catalysts. The reaction rate expression, derived from elementary steps of carbene mechanism, was identified by solving the inverse problem with step test data. The direct problem was solved by orthogonal collocation within the method of lines. Model predictions agreed with responses from dynamic experiments carried out under conditions different from those used for estimating model parameters.

Introduction

A suitable kinetic model is of fundamental importance in the design and optimization of catalytic reactors. Catalytic reactors are often modeled using macrokinetic analysis, which has several inherent limitations (Dumesic et al., 1993), whereas microkinetic analysis leads to a better understanding of the physicochemical processes and aids in catalyst development. Though microkinetics has been receiving attention recently, the effect of physisorption on reaction has received little or no attention. For reactions at conditions close to the equilibrium vapor pressure of the reactants and products, the effects due to physisorption are not negligible. This occurs for propene metathesis over Re_2O_7/γ-Al_2O_3 catalyst and for several other classes of reactions (such as isomerization) of industrial relevance.

Reaction kinetics are often derived from steady-state experiments, whereas transient experiments and dynamic models provide more information efficiently (Tamaru, 1978). Dynamic models enable improved control and optimization, safe startup and shutdown, enhanced performance with periodic inputs, and prediction of operating conditions. Transient experiments pose significant challenges in reaction engineering (Villadsen, 1988) due to difficulties with rapid analysis of reactor effluent, rapid generation of input forcing functions, input variable manipulation, constraints of safe operation, and real-time data processing. Further, data on multicomponent sorption-diffusion dynamics are limited (Hu and Do, 1992). In this article, we describe the characteristics of physisorption, diffusion and reaction in propene metathesis, dynamic models of a heterogeneous catalytic reactor, and tests for model prediction using a computer-controlled Berty reactor.

Correspondence concerning this article should be addressed to V. G. Gomes who is currently at the Dept. of Chemical Engineering, The University of Sydney, NSW 2006, Australia.

Reaction

Banks and Bailey (1964) first reported the discovery of metathesis reactions by which linear alkenes and alkynes are converted into equimolar amounts of lower and higher homologues. In propene metathesis, propene molecules are converted into equimolar amounts of ethene and 2-butene at ambient condition in the presence of Re_2O_7/γ-Al_2O_3 catalyst:

$$2CH_2=CH-CH_3 \rightleftarrows CH_2=CH_2+CH_3-CH=CH-CH_3$$

The first commercial propene metathesis plant was built in 1966 at Shawinigan Chemicals, Québec. The reverse reaction producing propene, as well as several other metathesis reactions have been identified as economically viable for manufacturing a wide range of valuable specialty chemicals (Short and Ramirez, 1987).

In this article, the kinetics expression for propene metathesis was based on elementary steps. The reaction mechanism

with nonpairwise exchange, first proposed by Hérisson and Chauvin (1970), was based on metal carbene intermediate formation—the methylidene ($M = CH_2$) and ethylidene ($M = CHCH_3$) complexes (where M denotes an active site):

Step 1: $C_3H_6 + M = CH_2 \rightleftarrows C_3H_6M = CH_2$
Step 1a: $C_3H_6M = CH_2 \rightleftarrows C_2H_4M = CHCH_3$
Step 2: $C_2H_4M = CHCH_3 \rightleftarrows C_2H_4 + M = CHCH_3$
Step 3: $C_3H_6 + M = CHCH_3 \rightleftarrows C_3H_6M = CHCH_3$
Step 3a: $C_3H_6M = CHCH_3 \rightleftarrows C_4H_8M = CH_2$
Step 4: $C_4H_8M = CH_2 \rightleftarrows C_4H_8 + M = CH_2$

The desorption steps have been shown to be the most likely rate-determining steps (Kapteijn et al., 1981), hence, with steps 2 and 4 as the rate-determining processes, the kinetic expression is given by

$$R_A = \frac{k_r K_P\left(y_P^2 - y_B y_E/K_{eq}\right)}{y_P + K_P y_P^2 + K_E y_E + K_B y_B + K_{PE} y_P y_E + K_{PB} y_P y_B}, \tag{1}$$

where

$$k_r = L_r k_2 k_4/(k_2 + k_4) \tag{2}$$

$$K_P = K_1 K_3 (k_2 + k_4)/(k_2 K_1 + k_4 K_3) \tag{3}$$

$$K_E = k_2/(k_2 K_1 + k_4 K_3) K_2 \tag{4}$$

$$K_B = k_4/(k_2 K_1 + k_4 K_3) K_4 \tag{5}$$

$$K_{PE} = k_2 K_1/(k_2 K_1 + k_4 K_3) K_2 \tag{6}$$

$$K_{PB} = k_4 K_3/(k_2 K_1 + k_4 K_3) K_4 \tag{7}$$

$$K_{eq} = K_1 K_2 K_3 K_4. \tag{8}$$

Model Equations

Our assumptions for the model equations describing propene metathesis dynamics in a Berty reactor are (a) well-mixed gas phase due to high internal recirculation ratio, $\Omega = 58$, measured for the reactor; (b) negligible mass transfer resistance at the gas–solid interface, concluded on measuring high mass transfer coefficient by naphthalene sublimation ($Bi_m \simeq 600$); (c) equilibrium condition at the gas–adsorbent interface due to rapid sorption (Kreuzer and Gortel, 1986); and (d) constant solid phase properties.

The mass and energy balances for each species in the adsorbed phase and the bulk gas phase are given by:

Adsorbed Phase:

$$\frac{\partial C_i}{\partial t} = 1/r^2 \frac{\partial}{\partial r}\left(r^2 \mathfrak{D}_{ei} \frac{\partial C_i}{\partial r}\right) + \vartheta \tag{9}$$

$$\rho_s C_{ps} \frac{\partial T_s}{\partial t} = k_s\left[\frac{\partial^2 T_s}{\partial r^2} + 2/r \frac{\partial T_s}{\partial r}\right] + (-\Delta H)\vartheta \rho_s. \tag{10}$$

Bulk Gas Phase:

$$V_R \frac{dy_i}{dt} = F(y_{if} - y_i) - 3\frac{V_c \rho_s (1-\epsilon_b)\, \mathfrak{D}_{ei}}{R_P} \frac{\partial C_i}{\partial r}\bigg|_{(R_P,t)} \tag{11}$$

$$V_R \rho_g C_{pg} \frac{dT_g}{dt} = F\rho_g C_{pg}(T_0 - T_g) - \frac{3V_c(1-\epsilon_b)k_s}{R_P} \frac{\partial T_s}{\partial r}\bigg|_{(R_P,t)}. \tag{12}$$

Initial Conditions:

$$C_i(r,0) = C_{i0} \tag{13}$$

$$y_i(0) = y_{i0} \tag{14}$$

$$T_s(r,0) = T_{s0} \tag{15}$$

$$T_g(r,0) = T_{g0}. \tag{16}$$

Boundary Conditions:

$$r^2 \partial C_i/\partial r \quad (0,t) = 0 \tag{17}$$

$$C_i(R_P,t) = f(P, y_E, y_P, y_B) \tag{18}$$

$$r^2 \partial T_s/\partial r \quad (0,t) = 0 \tag{19}$$

$$k_s \partial T_s/\partial r(R_P,t) = h_f(T_s - T_g). \tag{20}$$

In the preceding equations i denotes ethene (E), propene (P), or 2-butene (B); C_i denotes species concentration in the adsorbed phase; y_i is the species bulk gas phase concentration; T_s and T_g are the adsorbent and bulk gas phase temperatures, respectively. The species consumption or generation term, ϑ, in Eq. 9 represents $-R_A$ for propene, and $R_A/2$ for ethene and 2-butene, while in Eq. 10 ϑ represents $-R_A$.

Physisorption

The ideal adsorbed solution (IAS) theory (Myers and Prausnitz, 1965) was used for characterizing physisorption because of its thermodynamic consistency and successful application to steady-state multicomponent sorption (Valenzuela and Myers, 1989). The basic equation for IAS theory is analogous to Raoult's law for vapor–liquid equilibria:

$$P_T y_i = P_i^0(\pi_i) x_i, \tag{21}$$

where P_i^0 is the pressure, which, for the adsorption of pure component i, yields the same spreading pressure, π_i, as that of the mixture. The spreading pressure is defined by Gibbs adsorption isotherm

$$\pi_i A_s/R_u T = \int_0^{P_i^0} C_i^0(p)\, d(\ln p) \qquad i = 1, 2, \ldots, N, \tag{22}$$

where $C_i^0(p)$ is the adsorption isotherm of pure component. Among several isotherm equations (Yang, 1987), the extended Langmuir model was selected on finding little difference in its prediction ability compared to similar isotherm equations (such as, Toth), and for its computational ease (O'Brien and Myers):

$$C_i^0 = m_i\left[\eta_i/(1+\eta_i) + \sigma_i^2 \eta_i(1-\eta_i)/2(1+\eta_i)^3\right], \tag{23}$$

where $\eta_i = \kappa_i P_i^0$ and isotherm parameters are m_i, κ_i and σ_i.

An explicit relationship between π_i and P_i^0 from Eqs. 22 and 23 is

$$\Pi = \pi_i A_s / R_u T = m_i \left[\ln(1+\eta_i) + \sigma_i^2 \eta_i / 2(1+\eta_i)^2 \right]. \quad (24)$$

The adsorbed phase mole fractions, $x_i = P_i / P_i^0$ were added to give

$$\sum \kappa_i y_i R_u T / \left[\exp\left\{ \Pi / m_i - \sigma_i^2 \eta_i / 2(1+\eta_i)^2 \right\} - 1 \right] = 1 \quad (25)$$

Π was then determined from Eq. 25 by Newton–Raphson iteration using the spreading pressure for the component with the greatest sorption affinity as the starting value. Subsequently C_i was calculated from the computed x_i and the total amount adsorbed.

Diffusion

Effective diffusivities were calculated from molecular, Knudsen, and surface-diffusion coefficients. Molecular diffusivity, $\mathfrak{D}_{ij}$, of each component was estimated from the Chapman–Enskog equation (Satterfield, 1970) and combined with the Stefan–Maxwell relation to give diffusivity in a dilute mixture (Cussler, 1976):

$$\mathfrak{D}_{mi} = (1 - y_i) \left\{ \sum_i^N y_j / \mathfrak{D}_{ij} \right\}^{-1} \qquad (j \neq i). \quad (26)$$

Knudsen diffusivities (Satterfield, 1970) for catalyst meso- and macro-pores were calculated from:

$$\mathfrak{D}_{Ki} = 9{,}700\, r_e (T/M_i)^{1/2}. \quad (27)$$

For the transition regime, combined molecular and Knudsen diffusivities for the mixture, $\mathfrak{D}_{eu}$, were estimated by including contributions from the mesopore and macropore diffusion fluxes using the Wakao–Smith (1962) random-pore model.

Surface diffusivities were estimated from (Gilliland et al., 1974):

$$\mathfrak{D}_{Si} = 1.6 \times 10^{-6} \exp(-0.45\, q_i / R_u T) \quad (28)$$

and were incorporated into effective diffusivity through enhancement factors:

$$\chi_i = 1 + (2/r_e A_s)(\mathfrak{D}_{si}/\tau_s)/(\mathfrak{D}_{eu}/\tau_p) dC_i/dy_i, \quad (29)$$

where

$$dC_i/dy_i = m_i \kappa_i / (1 + \kappa_i P_i)^2 \left[1 + \{1 - 4\kappa_i P_i - \kappa_i^2 P_i^2\} / (1 + \kappa_i P_i)^2 \right]. \quad (30)$$

Equation 29 allows for concentration dependency of surface diffusivity for a single component; however, for multiple components, this dependence is simplified by ignoring the interaction of different adsorbed species. In other words, a diagonal Jacobian is used in the Darken relationship.

Table 1. Diffusivities of Ternary Adsorbates in Helium

Diffusivity (m^2/s)	C_2H_4-Mix	C_3H_6-Mix	C_4H_8-Mix
$\mathfrak{D}_{ij} \times 10^4$	0.2883	0.2519	0.2157
$\mathfrak{D}_{ei} \times 10^7$	0.5759	0.5018	0.4354

The pore and Knudsen diffusion tortuosity factors were assumed identical and were estimated from porosimetry data (Carniglia, 1986):

$$\tau_p = (2.23 - \phi_p \rho_p)[0.92(2\phi_p / r_e)/A_s]^{1+\mu}. \quad (31)$$

Surface diffusion tortuosity factor was estimated from (Ho and Strieder, 1981):

$$\tau_s = 6(1 - 0.5 \ln \epsilon_p)^2 / (9 - 2 \ln \epsilon_p). \quad (32)$$

The calculated pore and surface tortuosity factors, $\tau_p = 3.7$ and $\tau_s = 1.2$, are comparable to typical literature values. The slope, μ, of the logarithmic plot of $\mathfrak{D}_{eu}$ vs. r was determined to be 0.95, with the measured pellet porosity, $\epsilon_p = 0.4$ m^3/m^3. Surface diffusivities were based on the isosteric heat of adsorption ($q_E = 30$ kJ/mol, $q_p = 34$ kJ/mol, and $q_B = 38$ kJ/mol) for ethene, propene, and 2-butene (Tamon et al., 1981; Valenzuela and Myers, 1989). The corresponding enhancement factors, χ_i, were 1.18, 1.24, and 1.27 for 10% coverage. Effective diffusivities (typical values shown in Table 1) were calculated from

$$\mathfrak{D}_{ei} = \mathfrak{D}_{eu} \epsilon_p \chi_i / \tau_p. \quad (33)$$

Numerical Solution of Direct Problem

The differential-algebraic equations describing propene metathesis dynamics are nonlinear and coupled. Orthogonal collocation within the method of lines (OC-MOL) based on Jacobi polynomials was used for solving the differential equations (Villadsen and Michelsen, 1978). Four internal collocation points were tested sufficient for convergence after including the BC (Eqs. 17 and 19) symmetry: $u = r^2$. The ordinary differential equations (ODEs) were solved by Gear's stiff method along with the algebraic expressions (Gear, 1971) using variable-step variable-order backward differentiation formulas (DIVPAG, IMSL v.1.1).

The Jacobian matrix generated by forward finite difference was validated with analytical Jacobian for the linearized single component (LSC) model, and the OC-MOL numerical solutions were validated against analytical solutions (example in Appendix A) with linear sorption isotherm and kinetics. For the LSC model the numerical solutions matched the analytical solutions exactly (Figure 1) and agreed with measured responses (details in Gomes and Fuller, 1994a). The single component OC-MOL computations were then extended to multicomponent system, which proved to be stiff with maxi-

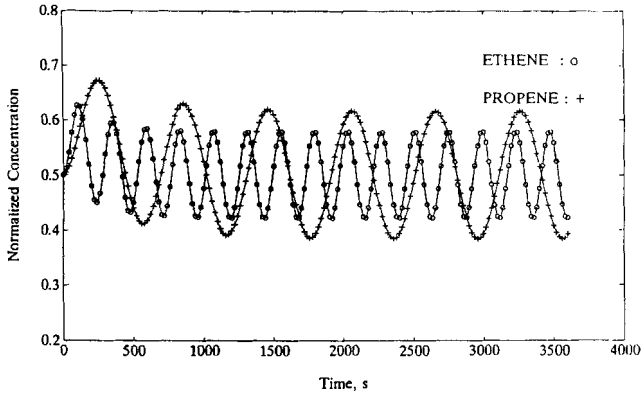

Figure 1. Comparison between OC-MOL (———) and analytical solutions (○, +) for sine wave inputs ($\omega_E = 0.02618$ rad/s, $\omega_P = 0.0105$ rad/s).

mum stiffness ratio $\xi \simeq 10^5$ (for stiff problems $\xi > 10^3$), where the stiffness ratio ξ = max |real (eigenvalue of J|/min |real (eigenvalue of J)|.

Experimental

The experimental work was carried out in several stages: development of experimental facility, morphological, and chemical characterization of catalyst pellets; determination of physisorption isotherms for ethene, propene, and 2-butene from steady-state experiments; determination of reaction kinetics from transient experiments; and transient sorption, diffusion, and reaction tests in a Berty reactor. The sorption-diffusion experiments were conducted with inactivated $Re_2O_7/\gamma\text{-}Al_2O_3$ pellets, and active catalysts were employed for reaction.

The facility for transient experiments (Figure 2) comprised a Berty reactor with a new impeller we developed for improved recirculation rate (by a factor of 2); adsorbent/catalyst; a revamped gas chromatograph (GC); a reactor effluent sampling system; four thermal mass flowmeters and controllers (FC280, Tylan, Carson, CA) for ethene, propene, 2-butene, and helium (each > 99.95% purity); a feed preheater; temperature and pressure instruments; and a data acquisition and control system.

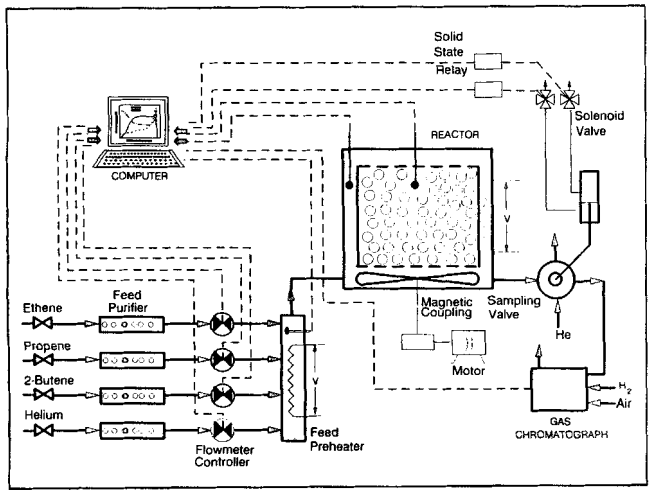

Figure 2. Experimental setup with microcomputer data acquisition and control system.

A Carle gas chromatograph (AGC-311), optimized for rapid analysis, received 50-μL reactor effluent every 22 s via a sampling valve actuated by solenoid valves and relays. The reactor temperature was controlled by a time-proportioning algorithm. Signals were acquired, filtered, peaks identified, processed, and stored every 10 ms. The details on measurement and interrupt-driven control are given elsewhere (Gomes, 1990; Gomes and Fuller, 1992).

For physisorption-diffusion experiments, the adsorbents were prepared by wet impregnation of γ-alumina pellets (3.175 mm in diameter and length) with ammonium perrhenate solution, followed by drying at 390 K and 28-mm Hg, and calcination at 850 K. The pellets were reduced in a stream of hydrogen for 6 h at 850 K (above the Tammann temperature) and tested for null catalytic activity from product stream analysis on exposure to propene. Absence of chemisorption on the reduced pellets was confirmed by measuring heat evolved on exposure to each adsorbate stream, with a differential scanning calorimeter (DSC, TAS7, Perkin-Elmer, Norwalk, CT). The measured BET surface area and pore volume were $A_s = 123.5$ m^2/g, $\phi_p = 0.472$ m^3/g.

For propene metathesis, the catalyst pellets were prepared by the wet impregnation method described earlier without the reduction step. The pellets were heated in dry air at 850 K for 2 h, and rinsed in dry helium for 4 h, also at 850 K, then the pellets were activated *in situ* with propene. The procedure gave consistent catalyst activity from batch to batch. The yellowish-white catalyst changed to deep purple on losing activity, which was restored on heating the pellets in dry air and then in helium at 850 K. The measured average BET surface area and pore volume were $A_s = 125.7$ m^2/g, $\phi_p = 0.470$ m^3/g. From the bimodal pore size distribution by nitrogen sorption and mercury porosimetry, the mesopore and macropore radii were 5.9 nm and 105.0 nm, respectively. The catalyst structural and chemical constitutions (Gomes, 1990) were determined by scanning electron microscopy (SEM) and electron spectroscopy for chemical analysis (ESCA).

Transient Physisorption Diffusion

Physisorption data from steady-state experiments at 298 K and 1 atm, conducted in a Flowsorb II apparatus (model 2300, Micromeritics, Norcross, GA), were fitted with extended Langmuir isotherm equations (Figure 3). The model parameters (Nonlin/BMDP routine) are given in Table 2. Model predictions were first tested for transient sorption-diffusion with single and then binary components for ethene, propene, and 2-butene, and were found to agree with experimental data (Gomes and Fuller, 1994b).

Ternary sorption-diffusion was characterized by increasing and decreasing step inputs of the primary components with constant secondary-component concentrations, using 15–25 g reduced $Re_2O_7/\gamma\text{-}Al_2O_3$ pellets; total gas flow rate, $F = 1.67 \times 10^{-6}$ m^3(STP)/s at 298 K and 101.325 kPa; reactor volume, $V_R = 2.174 \times 10^{-4}$ m^3; and bed porosity, $\epsilon_b = 0.39$ m^3/m^3. The total gas flow rate was held constant by on-line adjustment of inert gas (helium) flow rate. Species concentrations are reported as deviations from initial values and normalized with

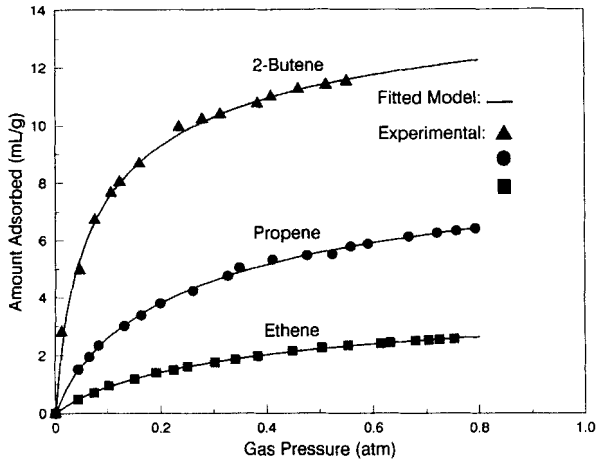

Figure 3. Sorption isotherms for ethene, propene, and 2-butene with fitted extended Langmuir models.

Table 2. Extended Langmuir Model Parameters

Parameter	Ethene	Propene	2-Butene
m_i (mol/kg)	0.1836 ± 0.0065	0.4106 ± 0.0154	0.8144 ± 0.1064
κ_i $(\text{MPa})^{-1}$	0.2397 ± 0.0018	0.3326 ± 0.0303	0.5140 ± 0.0113
σ_i	0.7263 ± 0.0075	0.8106 ± 0.1431	1.4244 ± 0.1774

malized with respect to the sum of initial to final deviations in concentrations.

Transient responses to ethene, propene, and 2-butene step inputs in ternary mixtures are shown in Figures 4, 5, and 6, respectively. For a propene step input, the gas phase concentration typically reaches 90% of the final value ($t_{0.9}$) in 580 s and 63% of the final value ($t_{0.63}$) in 250 s with mixture spreading pressure $\Pi_{PEB} = 0.392$ mol/kg. For steps in primary components, ethene step response is the fastest, while 2-butene response is the slowest of the three species. Propene has greater sorption affinity than ethene, hence, the desorbed amount of secondary components is higher for a step in propene than for a step in ethene. As 2-butene has greater

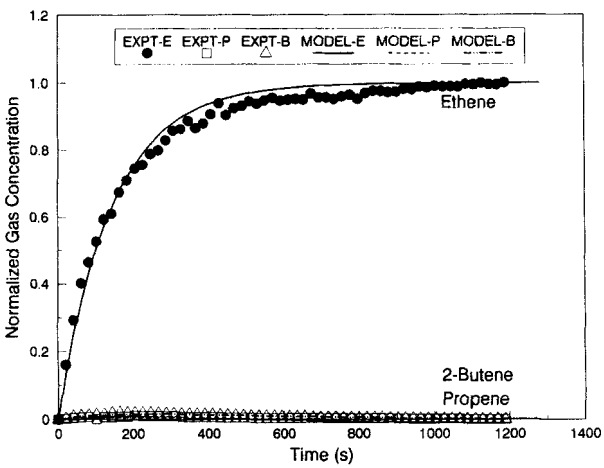

Figure 4. Step responses to ethene with ternary physisorption-diffusion.

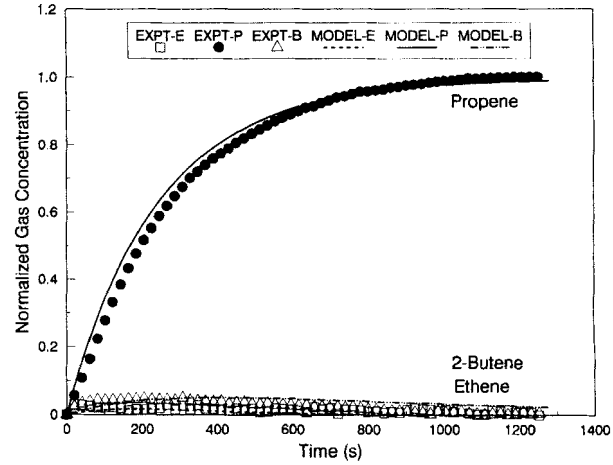

Figure 5. Step responses to propene with ternary physisorption-diffusion.

sorption affinity compared to ethene or propene, greater quantities of secondary components are desorbed for a 2-butene step. The theoretical predictions show reasonable agreement with the experiments. The primary and secondary component concentrations, and the primary step response times ($t_{0.9}$) are given in Table 3.

Reaction Kinetics: Inverse Problem

Parameter estimation in differential equations involves solving an inverse problem. Direct operator inversions in coupled nonlinear equations are difficult, thus the estimation was formulated as a nonlinear least squares problem (NLSP):

$$S_{ML} = \sum_{j}^{m} \sum_{i}^{n} [f_{ij}(X)]^2 w_{ij}, \tag{34}$$

where $f_{ij}(X)$ is the residual at time interval i for component j:

$$f_{ij}(X) = \left[y_{m_{ij}}(t) - y_{e_{ij}}(t) \right]. \tag{35}$$

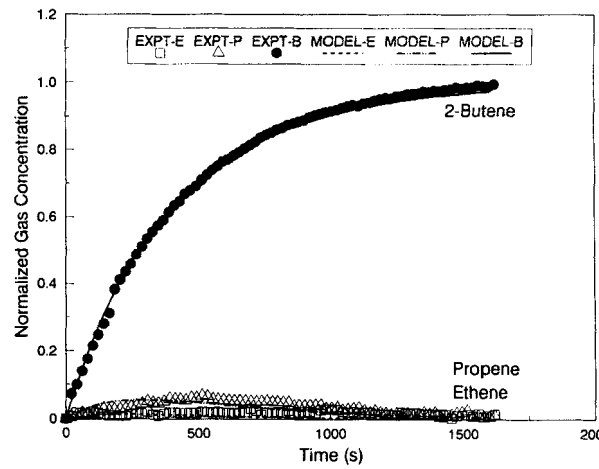

Figure 6. Step responses to 2-butene with ternary physisorption-diffusion.

Table 3. Experimental Parameters for Ternary System

Component	y_{i0}	y_{if}	y_{is}	$t_{0.9}$
$E-P-B$	4.09	4.90	3.90, 3.85	370
$P-E-B$	3.41	4.09	4.09, 2.06	580
$B-E-P$	4.30	5.16	4.09, 3.27	840

The choice of an optimal method for a general estimation problem or for a specific class of problems is yet unresolved, hence an exploration of this aspect was needed.

Initial use of direct or nongradient methods (Hooke and Jeeves, Rosenbrock algorithms) for an LSC system required a large number of iterations (about 100) for convergence. Use of unconstrained indirect or gradient methods (such as DUNLSF, IMSL v.1.1), resulted in function "blow-up" due to parameter excursions outside the feasible range. A packaged constrained nonlinear least squares algorithm, DBCLSF (IMSL v.1.1), was found inappropriate, because constrained parameters on reaching a boundary were transfixed, giving biased estimates for the remaining parameters.

The classic gradient-based approach to NLSP, the Gauss–Newton method, locally approximates changes in the objective function by a quadratic expansion, in which the Hessian matrix is approximated by J^TJ, where J is the Jacobian matrix. Gauss–Newton methods work well for Jacobians with full rank, therefore, most algorithms aim to exploit favorable behavior in Gauss–Newton methods whenever possible. The Levenberg–Marquardt (LM) method minimizes the Gauss–Newton quadratic model subject to trust-region constraint (Moré, 1978; Moré and Sorensen, 1983). Several implementations of this method exist. To solve the NLSP, the LM-QRD algorithm (LM with QR decomposition of J) with penalty function for inequality bounds was applied first (Moré, 1978), and was further refined by LM-SVD (LM with singular value decomposition of J) with active set strategy (Fletcher, 1980; Wright and Holt, 1985). The constrained NLSP is stated as follows:

$$\min_X \|f_{ij}(X)\|_2^2 \qquad \text{subject to} \quad C_j(X) \geq 0, \tag{36}$$

where $C_j(X)$ are positivity bounds based on thermodynamic constraints on kinetic parameters (Boudart, 1968). The covariance matrix was calculated from the Jacobian matrix (J):

$$\text{COV}(X) = (J^TJ)^{-1} = P(R^TR)^{-1}P^T, \tag{37}$$

where, the permutation matrix P and the upper triangular matrix R are from the QR decomposition: $JP = QR$.

Propene metathesis is mildly exothermic, hence the temperature rise of the bulk gas phase measured every 10 s, was 1–1.5 K, and the temperature difference between the catalyst and the gas phase was about 1 K. To estimate the thermal effect, characteristic properties (Table 4) of a packed bed were used (Doraiswamy and Sharma, 1984). The nonisothermal model equations were solved by the OC-MOL scheme. For a 20% step in propene concentration, model predictions show a similar trend as the measured gas phase temperature profile (Figure 7) with deviations arising from unaccounted reactor heat loss. Due to the small thermal effects, these were not included in subsequent calculations.

Table 4. Typical System Properties

$\rho_s = 870$ kg/m^3	$C_{ps} = 1.41$ kJ/kg·K
$\rho_g = 0.629$ kg/m^3	$C_{pg} = 5.12$ kJ/kg·K
$k_s = 5.8\times10^{-3}$ kJ/m·s·K	$h_f = 0.065$ kJ/m^2·s·K

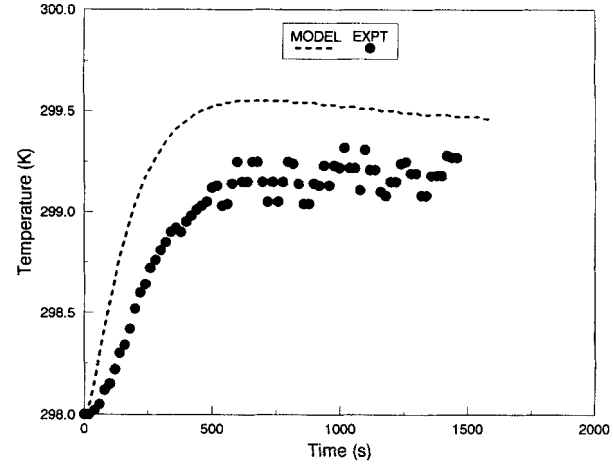

Figure 7. Gas-phase temperature profile for step in propene.

Propene step test data were used for estimating the kinetic parameters k_2, k_4, K_1, K_2, K_3, and K_4. Constraint boundaries were encountered several times with ill-conditioned variance-covariance matrix. Especially, variances for two parameters were unacceptably high ($>10^4$), indicating mutual dependence between parameters and suggesting $K_1 = K_3$, $k_2 = k_4$. On using these, the LM-QRD algorithm converged within fifteen iterations with acceptable residual sum of squares. The LM-SVD method also converged with parameters within 95% of those obtained by LM-QRD. The SVD showed no rank deficiency with positive-definite Hessian matrix. The estimated parameters with 95% confidence limits are given in Table 5.

Typical responses to step increase in propene concentration is shown in Figure 8 (step size = 0.65 mol/m^3, initial concentration = 3.27 mol/m^3). At steady state, propene concentration corresponds to about 72% of the step input, that is, 28% of propene is converted to ethene and 2-butene. For propene $t_{0.9} = 600$ s and $t_{0.63} = 240$ s, while for ethene $t_{0.9} = 400$ s and for 2-butene $t_{0.9} = 1{,}000$ s. The overall rate expression is given by

$$R_A = \frac{6.340\times10^{-2}(y_P^2 - y_B y_E/0.0397)}{y_P + 0.172y_P^2 + 2.309y_E + 2.727y_B + 0.398y_Py_E + 0.469y_Py_B} \tag{38}$$

Table 5. Estimated Kinetic Parameters

Parameters	Values	Confidence Intervals	Sensitivity Bounds
$L_r k_2$ (mol/s·kg)	0.00736	0.00046	5.225×10^{-4}
K_1 (m^3/mol)	0.17228	0.00385	1.347×10^{-7}
K_2 (mol/m^3)	1.25673	0.02197	4.865×10^{-6}
K_4 (mol/m^3)	1.06434	0.05335	2.526×10^{-4}

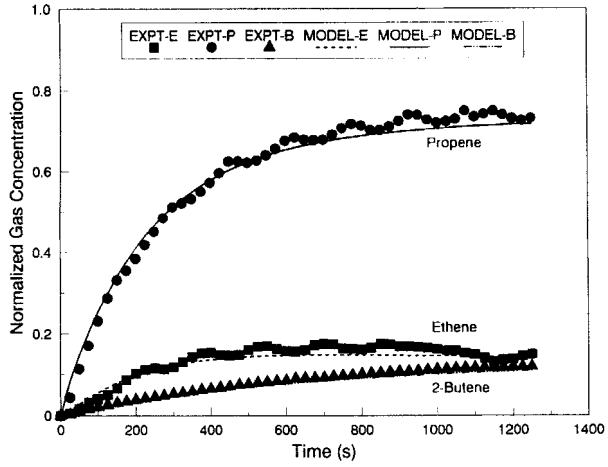

Figure 8. Responses to step increase in propene for reaction kinetics.

The denominator terms show greater weightage for 2-butene chemisorption than for ethene. The parameter sensitivity bounds were estimated from:

$$\zeta_i = \epsilon^{1/2} \| f_{ij}(X) \| / \| [\partial f_{ij}(X)/\partial X] \|, \tag{39}$$

where, $\epsilon = \sqrt{(\text{computer precision})} = 0.14 \times 10^{-7}$. If ζ_i is large relative to a parameter X, then the residual norm $f_{ij}(X)$ is insensitive to changes in X, indicating deficiency in estimation. The computed sensitivity bounds, Table 5, show that the residual norm is sensitive to changes in all the parameters.

The equilibrium constant, K_{eq}, from (TRC, 1985):

$$K_{eq} = \exp[-\Delta G^0(T)/R_u T] \tag{40}$$

was estimated to be 0.0415, which agrees with experimental data (Eq. 38).

Determination of active sites from poisoning experiments was precluded by the possibility of incapacitating the GC by catalyst probes: NO, N_2O, H_2O, and so on. Thus, the number of active sites, L_r, was obtained from the overall reaction rate constant, $L_r k_2$, and from the Arrhenius rate equation (Benson, 1976):

$$k_i = A \exp(-E_a/R_u T)$$
$$= (k_B T\ e/h) \exp(\Delta S/R_u) \exp(-E_a/R_u T). \tag{41}$$

The following were calculated from the transition state theory (details in Appendix B): frequency factor, $A = 5.3 \times 10^7$ s^{-1}; activation entropy loss, $\Delta S = -105.4$ J/mol·K; rate constant $k_i = 5.1$ s^{-1}; activation energy, $E_a = 40$ kJ/mol (agrees with data from Kapteijn et al., 1981). Thus active site density is 10^{16} m^{-2}, that is, about 1% of the rhenium atoms act as active sites. Hence the turnover frequency is about 1.0 s^{-1} per active site, and the amount of propene chemisorbed for reaction is 1.4×10^{-3} mol/kg, which is lower than the total amount physisorbed by a factor of 300.

Tests for Reaction, Diffusion, and Physisorption

The models were tested under conditions different from the ones for which the model parameters were obtained. Responses to a 20% step decrease in propene (Figure 9) at $y_{i0} = 4.66$ mol/m^3, exhibit behavior similar to those for a stepup with about 28% propene conversion. Ethene gradually reduces in concentration after reaching steady state in 800 s. This is due to desorption of 2-butene from the catalyst, which then adsorbs part of the ethene. The model predictions are in good agreement with experimental data.

Figure 10 shows responses to a propene sine input with 0.013 rad/s frequency and 0.87 mol/m^3 amplitude at 4.35 mol/m^3 propene concentration. The initial transient is dissipated within three cycles to give a steady-state propene amplitude ratio of 0.12 with respect to the input. The fundamental frequency of 0.013 rad/s and the amplitudes were verified by applying the fast Fourier transform. Theoretical predictions agree with experimental data with some deviations at the initial transient, due to disruption while introducing the sine forcing function.

Reactor transient responses in the absence of physisorption and diffusion were simulated using the kinetics equation with the mass balances. Figure 11 shows responses for the

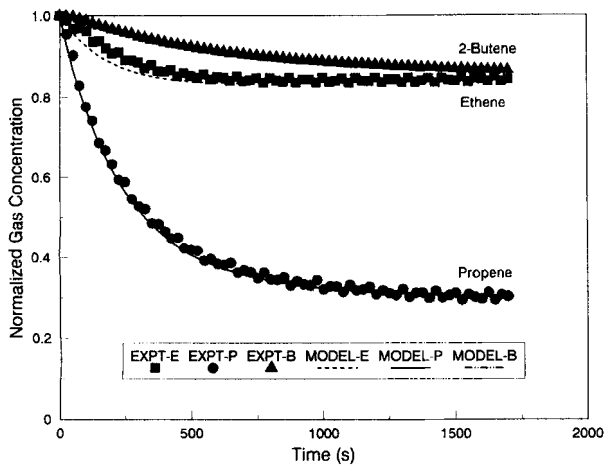

Figure 9. Responses to step decrease in propene including reaction, diffusion, and physisorption.

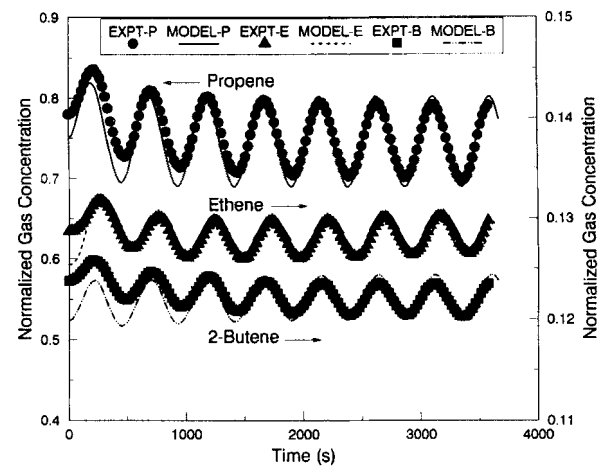

Figure 10. Responses to sine wave input in propene.

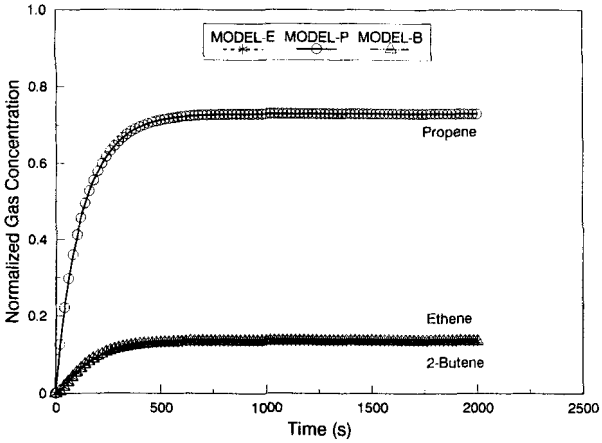

Figure 11. Simulation of responses for step increase in propene with reaction and without physisorption-diffusion.

same conditions as Figure 8. The final steady-state concentration levels for each of the components are correctly predicted; however, the responses for ethene and 2-butene merge completely (symbols plotted for distinction), with all components reaching steady state in 400 s in contrast to responses in Figures 8 and 9. Hence, excluding physisorption and diffusion result in substantial error in response prediction, which adversely affects kinetic parameter determination.

With zero initial concentration and a propene step of 4.09 mol/m^3, the responses (Figure 12) are significantly slower compared to steps from a nonzero initial concentration (Figure 8 and all previous responses) due to greater initial loading. For propene $t_{0.9} = 1{,}500$ s and $t_{0.63} = 600$ s, while $t_{0.9} = 3{,}000$ s for 2-butene and 750 s for ethene. The reequilibration of ethene on 2-butene desorption is noticeable. These predictions would have been grossly in error had physisorption been neglected.

Conclusions

Propene metathesis on rhenium oxide/γ-alumina catalyst was characterized for the simultaneous effects due to multi-component physisorption, diffusion, and reaction. The model equations included the IAS theory for multicomponent physisorption, Knudsen, molecular, and surface diffusivities for catalyst with bimodal pore size, and reaction kinetics based on carbene mechanism. An experimental strategy was developed to decouple the effects due to physisorption and reaction. Sorption isotherms from steady-state experiments with inactive catalysts were used to characterize transient sorption diffusion.

The direct problem was solved by orthogonal collocation within the method of lines (OC-MOL), and the inverse problem was solved by the constrained Levenberg–Marquardt algorithm with stable *QR* and *SV* decompositions of the Jacobian. The kinetic parameters were estimated from transient experiments in a computer-controlled Berty reactor. Four parameters were found to be independent and sufficient to describe the kinetics. The number of active sites was estimated as 1% of rhenium atoms in the catalyst. The average amount of propene chemisorbed was computed to be smaller than the amount physisorbed by a factor of 300.

Model predictions tested against experiments under conditions different from those used for obtaining the parameters showed reasonable agreement. The effect of physisorption was found to be significant in heterogeneous catalysis when the reaction conditions are close to the equilibrium vapor pressures of the reactants and products. Hence neglecting sorption-diffusion while identifying reaction kinetics can lead to substantial error.

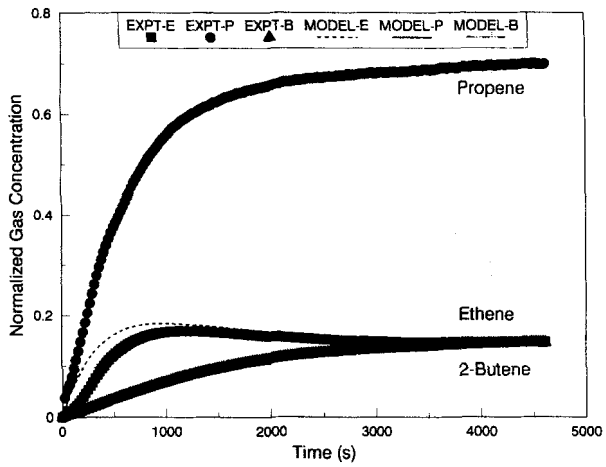

Figure 12. Responses to step increase in propene at zero initial concentration with reaction, diffusion, and physisorption.

Acknowledgments

Financial support of this work by McGill Major Fellowship and Bowen Fuller Fellowship is gratefully acknowledged.

Notation

Bi_m = mass transfer Biot number
c = velocity of light, m/s
C = adsorbed phase concentration, mol/kg adsorbent
C_{i0} = initial adsorbed phase concentration, mol/kg adsorbent
C_{pg} = specific heat of gas, kJ/kg K; C_{ps} (catalyst)
F = reactor inlet gas flow rate, m^3/s
ΔG = change in Gibbs free energy, kJ/mol
h = Planck's constant, 6.6242×10^{-34} J·s
h_f = film heat transfer coefficient, kJ/m^2·s·K
k_B = Boltzmann constant, 1.3805×10^{-23} J/K
k_r = overall reaction rate constant, mol/kg·s
k_S = catalyst thermal conductivity, kJ/m·s·K
K_i = equilibrium constant of elementary reaction i
K_X = chemisorption equilibrium constant of process
M_i = molecular weight of species, g/gmol
N = number of components in gas phase
P_i = partial pressure of species in gas phase, kPa
P_T = total pressure, kPa
q_i = isosteric heat of adsorption, kJ/mol
Q = orthogonal matrix in *QR* decomposition
r = radial dimension, m
r_e = effective average pore radius, m
R_A = reaction rate expression
R_P = pellet radius, m
R_u = universal gas constant, 8.3130 J/mol·K
S_{ML} = Euclidean norm of residual vectors
t = time, s
T = mean temperature, K
V_C = catalyst volume, m^3
V_R = reactor circulating gas and bed interstitial volume, m
w_{ij} = weighting matrix
x_i = mole fraction in the adsorbed phase

y_{i0} = initial gas concentration, mol/m^3 gas; y_{is} (secondary species)
y_{if} = gas phase input concentration at reactor inlet, mol/m^3 gas
y_e = measured value of dependent variable; y_m (predicted value)

Greek letters

η_i = transformed pressure of species
ρ_g = density of gas, kg/m^3; ρ_s (solid)
σ_e = external symmetry number of molecule
ψ = slope of adsorption isotherm, m^3 gas/kg adsorbent
Ω = reactor recirculation ratio

Literature Cited

Banks, R. L., and G. C. Bailey, "Olefin Disproportionation: A New Catalytic Process," *Ind. Eng. Chem. Prod. Res. Dev.*, **3**, 170 (1964).
Benson, S. W., *Thermochemical Kinetics*, 2nd ed., Wiley, New York (1976).
Boudart, M., *Kinetics of Chemical Processes*, Prentice-Hall, Englewood Cliffs, NJ (1968).
Carniglia, S. C., "Construction of the Tortuosity Factor," *J. Catal.*, **102**, 401 (1986).
Cussler, E. L., *Multicomponent Diffusion*, Elsevier, Amsterdam (1976).
Doraiswamy, L. K., and M. M. Sharma, *Heterogeneous Reactions: Analysis, Examples and Reactor Design*, Vol. 1, Wiley, New York (1984).
Dumesic, J. A., D. F. Rudd, L. M. Aparicio, and J. M. Rekoske, *The Microkinetics of Heterogeneous Catalysis*, American Chemical Society, Washington, DC (1993).
Fletcher, R., *Practical Methods of Optimization*, Wiley, New York (1980).
Gear, C. W., *Numerical Initial Value Problems in Ordinary Differential Equations*, Prentice-Hall, Englewood Cliffs, NJ (1971).
Gilliland, E. R., R. F. Baddour, G. P. Perkinson, and K. J. Sladek, "Diffusion on Surfaces," *Ind. Eng. Chem. Fundam.*, **13**, 95 (1974).
Gomes, V. G., "Physisorption and Diffusion in Propene Metathesis," PhD Thesis, McGill University, Montréal, P.Q., Canada (1990).
Gomes, V. G., and O. M. Fuller, "Computer Control for the Study of Reactor Dynamics," *Anal. Instrum.*, **20**, 183 (1992).
Gomes, V. G., and O. M. Fuller, "Periodic and Nonperiodic Dynamic Responses for Sorption Diffusion and Reaction in a Berty Reactor," *Ind. Eng. Chem. Res.*, **33**, 102 (1994a).
Gomes, V. G., and O. M. Fuller, "Fixed-Bed Adsorber Dynamics in Binary Physisorsorption Diffusion," *Can. J. Chem. Eng.*, **72**, 622 (1994b).
Hérisson, J. L., and Y. Chauvin, "Catalysis of Transformation of Olefins by Tungsten Complexes," *Makromol. Chem.*, **141**, 161 (1970).
Ho, F. G., and W. Strieder, "A Variational Calculation of the Effective Surface Diffusion Coefficient and Tortuosity," *Chem. Eng. Sci.*, **36**, 253 (1981).
Hu, X., and D. D. Do, "Multicomponent Adsorption Kinetics of Hydrocarbons to Activated Carbon," *Chem. Eng. Sci.*, **47**, 1715 (1992).
Kapteijn, F., H. L. G. Bredt, E. Homburg, and J. C. Mol, "Kinetics of the Metathesis of Propene," *Ind. Eng. Chem. Prod. Res. Dev.*, **20**, 457 (1981).
Kreuzer, H. J., and Z. W. Gortel, *Physisorption Kinetics*, Springer-Verlag, Berlin (1986).
Moré, J. J., "The Levenberg-Marquardt Algorithm: Implementation and Theory," *Proc. Dundee Conf. on Numer. Analysis*, G. A. Watson, ed., Springer-Verlag, Berlin, p. 105 (1978).
Moré, J. J., and D. C. Sorensen, "Computing a Trust Region Step," *SIAM J. Sci. Stat. Comp.*, **4**, 553 (1983).
Myers, A. L., and J. M. Prausnitz, "Thermodynamics of Mixed-Gas Adsorption," *AIChE J.*, **11**, 121 (1965).
O'Brien, J. A., and A. L. Myers, "Rapid Calculations of Multicomponent Adsorption Equilibria from Pure Isotherm Data," *Ind. Eng. Chem. Process Des. Dev.*, **24**, 1188 (1985).
Satterfield, C. N., *Mass Transfer in Heterogeneous Catalysis*, MIT Press, Cambridge, MA (1970).
Short, H., and R. Remirez, "Disproportionation Process Widens Its Commercial Scope," *Chem. Eng.*, **94**(11), 22 (1987).
Tamaru, K., *Dynamic Heterogeneous Catalysis*, Academic Press, London (1978).
Tamon, H., S. Kyotani, H. Wada, M. Okazaki, and R. Toei, "Surface Flow Phenomenon of Adsorbed Gases on Activated Alumina," *J. Chem. Eng. Japan*, **14**, 136 (1981).
TRC Thermodynamic Tables — Hydrocarbons, Vol. 8, Thermodynamics Research Center, Texas A&M University System, College Station, TX (1985).
Valenzuela, D. P., and A. L. Myers, *Adsorption Equilibrium Data Handbook*, Prentice-Hall, Englewood Cliffs, NJ (1989).
Villadsen, J., and M. L. Michelsen, *Solution of Differential Equation Models by Polynomial Approximation*, Prentice-Hall, Englewood Cliffs, NJ (1978).
Villadsen, J., "Challenges and Cul-de-sacs in Reactor Modelling," *Chem. Eng. Sci.*, **43**, 1725 (1988).
Wakao, N., and J. M. Smith, "Diffusion in Catalyst Pellets," *Chem. Eng. Sci.*, **17**, 825 (1962).
Wright, S. J., and J. N. Holt, "Algorithms for Nonlinear Least Squares with Linear Inequality Constraints," *SIAM J. Sci. Stat. Comp.*, **6**, 1033 (1985).
Yang, R. T., *Gas Separation by Adsorption Processes*, Butterworths, Boston (1987).

Appendix A

The dimensionless sorption-diffusion equations are

$$\epsilon_R\,\partial\tilde{C}/\partial\tilde{t} = (1/\tilde{r}^2)\,\partial/\partial\tilde{r}(\tilde{r}^2\partial\tilde{C}/\partial\tilde{r}) \tag{A1}$$

$$d\tilde{y}/d\tilde{t} = \tilde{y}_f - \tilde{y} - (3/\epsilon_C)(\partial\tilde{C}/\partial\tilde{r})|_{(\tilde{r}=1)} \tag{A2}$$

$$\tilde{C}(r,0) = 0; \qquad \tilde{y}(\tilde{t}=0) = 0 \tag{A3}$$

$$\tilde{r}^2\partial\tilde{C}/\partial\tilde{r}\,(0,\tilde{t}) = 0; \qquad \tilde{C}(1,t) = \psi(\Delta y/\Delta C)\tilde{y}, \tag{A4}$$

where the dimensionless parameters are

$$\tilde{r} = r/R_P; \qquad \tilde{t} = Ft/V_R; \qquad \tilde{C} = (C - C_0)/\Delta C;$$

$$\tilde{y} = (y - y_0)/\Delta y; \qquad \epsilon_R = FR_P^2/V_R\,\mathfrak{D}_{ei};$$

$$\epsilon_C = FR_P^2(\Delta y/\Delta C)/V_C\,\rho_s(1-\epsilon_b)\,\mathfrak{D}_{ei}$$

$$\text{and} \qquad \Delta y = y_f - y_0, \quad \Delta C = C_f - C_0.$$

The analytical solution of the preceding equations for a sine wave input, $\tilde{y}_f = A\sin(\omega\tilde{t})$ of amplitude A and frequency ω, is given by

$$\tilde{y} = \sum_{n=1}^{\infty} \frac{A\,\omega\exp(-\lambda_n^2\tilde{t}/\epsilon_R)}{\left[(\lambda_n^2/\epsilon_R^2)^2 + \omega^2\right]\left[1 + 1.5\psi\,\epsilon_R/\epsilon_C\left(1 + \cot^2\lambda_n - \frac{1}{\lambda_n}\cot\lambda_n\right)\right]}$$

$$+ 1/\sqrt{(\alpha^2+\beta^2)}\,\sin(\omega\tilde{t} - \tan^{-1}\beta/\alpha) \tag{A5}$$

where,

$$\alpha = \left[1 + 3\psi/\epsilon_C\frac{\coth\gamma(\gamma\csc^2\gamma - \coth\gamma) + \cot\gamma(\gamma\,\mathrm{csch}^2\gamma - \cot\gamma)}{\coth^2\gamma + \cot^2\gamma}\right]$$

$$\beta = \left[\omega + 3\psi/\epsilon_C \frac{\gamma(\coth\gamma \csc^2\gamma - \cot\gamma \operatorname{csch}^2\gamma)}{\coth^2\gamma + \cot^2\gamma} \right]$$

$$\gamma = \sqrt{(\epsilon_R \omega/2)},$$

where λ_n is the solution of

$$1 + \lambda/\epsilon_R + 3\psi/\epsilon_C(\lambda \coth\lambda - 1) = 0.$$

Appendix B

The estimation of rate and equilibrium constants was based on thermodynamic functions of the reacting species and equations from statistical mechanics (Benson, 1976; TRC, 1985). The entropy loss was based on the formation of transition state, metallocyclobutane (*TS*), from the reactant (*P*) and the alkylidene intermediate (*e*):

$$\Delta S = S^0_{TS} - S^0_P - S^0_e. \tag{B1}$$

Standard translation entropy for 2 degrees of freedom:

$$S^0_{\text{2D-trans}} = R_u[1.5\ln(M_i T a_s) + 33.1]. \tag{B2}$$

Standard rotation entropy for 2 degrees of freedom:

$$S^0_{\text{2D-rot}} = R_u[\ln(T) + \ln(I) - \ln(\sigma_e) + 89.4]. \tag{B3}$$

Entropy contribution for each vibration frequency of a molecule:

$$S^0_{\text{vib}} = -\ln[1 - \exp(-x_c)] + x_c/[\exp(x_c) + 1] \tag{B4}$$

$$x_c = ch\nu/k_B T. \tag{B5}$$

The vibrational contributions for stretching and deformation were calculated from the average wave number, ν, and the unknown deformation wave numbers were estimated from known values for similar compounds:

$$\nu_1/\nu_2 = [M_2/M_1]^{1/2}. \tag{B6}$$

The entropy loss was calculated as follows:

(a) Translation loss of propene (2° of freedom) = −96.9 J/mol·K (based on 1 wt. % of active sites available, $a_s = 3.9 \times 10^{-18}$ m^2 per molecule)

(b) Rotation loss of propene (2° of freedom) = −47.4 J/mol·K (based on the harmonic mean of the moments of inertia, $I = 15.2 \times 10^{-36}$ g·m^{-2}; $\sigma_e = 1$)

(c) Stretching vibrations for C = C (1,650 cm^{-1}) to C − C (1,000 cm^{-1}) = 0.4 J/mol·K

(d) Stretching vibrations for C = M (1,650 cm^{-1}) to C − M (419 cm^{-1}) = 3.7 J/mol·K

(e) Vibrations within single bonds C − C (1,000 cm^{-1}) = 0.4 J/mol·K

(f) Vibrations within single bonds C − M (419 cm^{-1}) = 3.8 J/mol·K

(g) In-plane deformation of metallocyclobutane intermediate (*TS*), based on two bends in C − C − M (306 cm^{-1}) and one bend in C − C − C (420 cm^{-1}) = 15.3 J/mol·K

(h) Out-of-plane bending of *TS*, based on two bends in C − C − M (306 cm^{-1}) and one bend in C − C − C (420 cm^{-1}) = 15.3 J/mol/K

(i) Total entropy change, ΔS = −105.4 J/mol·K

The intrinsic activation energy of an elementary reaction is a measure of the amount by which the electron clouds of the reactants must be deformed to permit the reaction to proceed. An empirical approximate relation for metathesis reactions is given by (Benson, 1976):

$$E_a = 4.18(14.8 - 3.64 I_e)/(1 + \Delta H/40), \tag{B7}$$

where the heat of reaction, $\Delta H = 14.1$ kJ/mol and the electron affinity, $I_e = 0.5$ eV (TRC, 1985; Benson, 1976).

Manuscript received Oct. 11, 1994, and revision received Dec. 27, 1994.